Kozai migration with tidal friction (KCTF) as a source for Gliese 436b's eccentricity

Hervé Beust, Xavier Bonfils, Xavier Delfosse, Thierry Forveille

UJF-Grenoble 1 / CNRS-INSU, Institut de Planétologie et d'Astrophysique de Grenoble (IPAG) UMR 5274

B.P. 53, F-38041 Grenoble Cedex 9 (France)

1 The Gliese 436 system

- The M-dwarf GJ 436 is a rare example of extrasolar system with a transiting Neptune-sized planet, GJ 436b (Butler et al. 2004, Gillon et al. 2007). It is a small period planet ($P = 2.64$ days, $a = 0.0287$ AU; Ballard et al. 2010) with a significant orbital eccentricity: $e \simeq 0.14 \pm 0.01$ (Maness et al. 2007; Demory et al. 2007).
- This eccentricity is surprisingly high. Tidal forces are expected to circularize the orbit within $\sim 10^7 - 10^8$ yr, i.e., much less than the present age of the system (1–10 Gyr, Torres et al. 2007).
- Many theories were proposed in recent years to account for the eccentricity of GJ 436b:
  1– The planet is not yet circularized due to weak tides, i.e., a large tidal dissipation parameter Q_p ($> 10^6$), while the standard typical values are a few 10^5 (Mardling 2008)
  2– The eccentricity is sustained by gravitational perturbations by an outer massive planet. This is not a straighforward explanation, as in all cases tides inevitably lead to damp all the eccentricity modulation and to circularize the orbit. Batygin et al. (2009) found that this effect can be considerably delayed if the planets initially lie at specific stationary points in phase space.
- In this work, we present an alternate model involving Kozai resonance with tidal friction (KCTF, Fabrycky & Tremaine 2007) to explain the present eccentricity of GJ 436b in spite of tidal forces. Computations were performed using the symplectic code for hierarchical systems HJS (Beust 2003) to which we have added tidal interaction and first order relativistic correction.

2 The Kozai resonance

- Kozai mechanism (or resonance) was first described by Kozai (1962), initially for comets on inclined orbit ($\gtrsim 40°$) with respect to the ecliptic (Bailey et al. 1992). Under the effect of secular perturbations (mainly arising from Jupiter), their orbit is subject to a periodic evolution that drives them to lower inclination but very high eccentricity, while the semi-major axis remains constant. An outer planet perturbing GJ 436b this way could trigger eccentricity variations.
- But if we take into account the tidal forces (here with $Q_p = 10^5$, a standard value) and the relativistic precession, the eccentricity modulation disappears (Fig. 1). A regular tidal circularization process starts instead with $t_{\rm circ} \simeq 2.3 \times 10^8$ yr, which is still short compared to the age of the system. **Consequently, Kozai resonance cannot account *this way* for the present eccentricity of GJ 436b.**

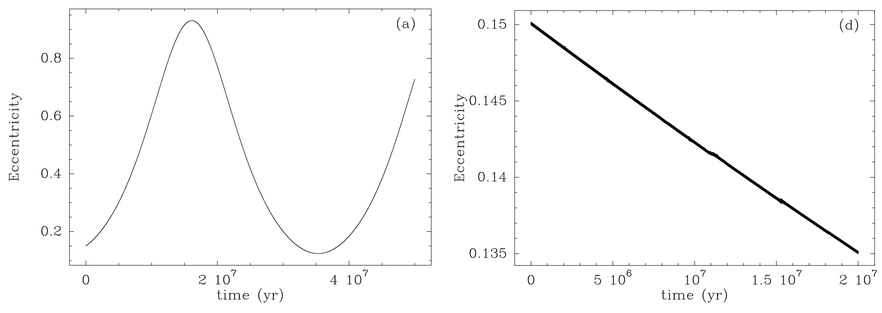

Figure 1 Example of eccentricity evolution of GJ 436b starting on its present-day orbit under the effect of Kozai resonance with a 0.1 $M_{\rm Jup}$ planet located at 3.6 AU (Orbital period = 10 yrs) from the star with an initial orbital inclination of 75° with respect to GJ 436b, with no tides and no relativistic precession (left), and with tides and relativity taken into account (right). In the latter case, there are no Kozai cycles anymore

3 The Kozai migration scenario

I - Short term bahaviour

- The problem can be solved if we assume that GJ 436b used to orbit the star initially further out than today (5–10 times, i.e. 0.15–0.3 AU), still in the presence of an inclined perturber involving KCTF. With $a = 0.287$ AU and the same perturber (0.1 $M_{\rm Jup}$ at 3.6 AU, inclination 75°), then the relativistic precession and the tides are too weak to prevent the onset of Kozai cycles (see Fig. 2).
- In the high eccentricity phases of the Kozai cycles, the periastron is now small enough to let tidal forces act. The first effect is a rapid spin synchronization of the planet with its orbital velocity *at periastron*. This results in a spinning up of the planet (Fig. 2).
- At periastron, the tidal friction induces a gradual decay of the semi-major axis of GJ 436b (Fig. 2). As this process is only active in the high eccentricity phases of the Kozai cycles, the decrease of the semi-major axis shows a characterisitic stair-case like evolution.

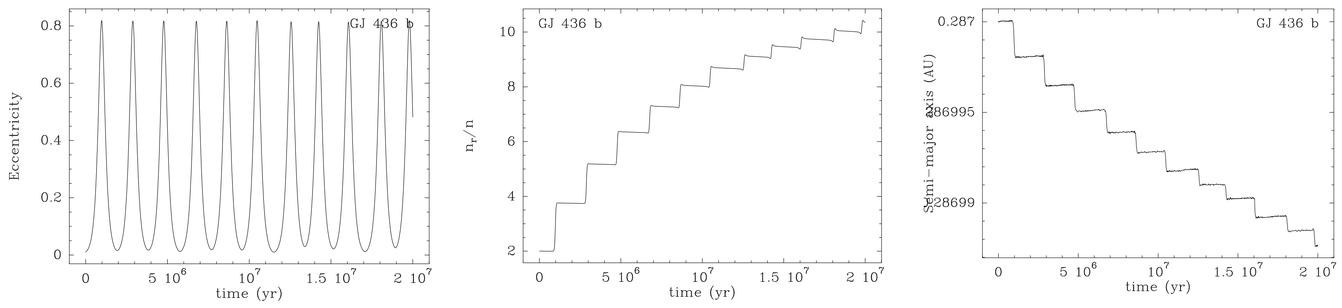

Figure 2 : Short term orbital evolution of GJ 436b initially put 10 times further out than today (0.287 AU), under the effect of Kozai resonance with a 0.1 $M_{\rm Jup}$ planet located at 3.6 AU from the star with an initial inclination of 75°. **Left :** Eccentricity evolution, showing Kozai cycles in agreement with theoretical predictions; **Middle :** Evolution of the ratio of the spin velocity of GJ 436b to its orbital mean motion (1 means synchronism). The planet's rotation is accelerated due to synchronization at periastron; **Right :** Evolution of the semi-major axis. We note a small staircase-like decay due to tidal friction

II - Long term behaviour

- On a longer time span (20 Gyr here) the secular evolution of GJ 436b appears twofold, with two distinct phases, already described by Fabrycky & Tremaine (2007) as characteristic for KCTF : **The first phase** is characterized by Kozai cycles (Fig. 3), a slow decay of the semi-major axis, and a gradual increase of the bottom eccentricity of the cycles. In **the second phase**, the planet leaves the Kozai resonance and starts a more rapid orbital decay and a circularization. Simultaneously the mutual inclination stabilizes to a smaller value. The transition time between the two phases corresponds to the point where the bottom eccentricity of the Kozai cycles reaches the top one. This process known as Kozai migration was pointed out by Nagasawa et al. (2008) as a way to generate close-in planets.
- Noticeably, the global timescale of the whole process is considerably longer than the basic tidal circularization timescale. Moreover, once the second phase starts, the decrease of the semi-major axis is much more rapid than that of the eccentricity. Hence we come to a state where the semi-major axis has already reached its present-day value while the eccentricity is still significant. **This way we may explain the present-day eccentricity of GJ 436b**
- The slow decrease of the eccentricity in the second phase could appear surprising, as the planet has now left Kozai resonance. This is in fact related to a stationary eccentricity configuration comparable to that described by Batygin et al. (2009), who showed that starting from an apsidal fixed point characterized by $de/dt = 0$, the tidal decrease of the eccentriciy is much slower. Here at the end of the first phase, we exactly come to a stationary configuration in eccentricity, as the bottom eccentricity of the Kozai cycles equals the peak one. This results in a huge increase (by a factor ~ 50) of the circularization time.

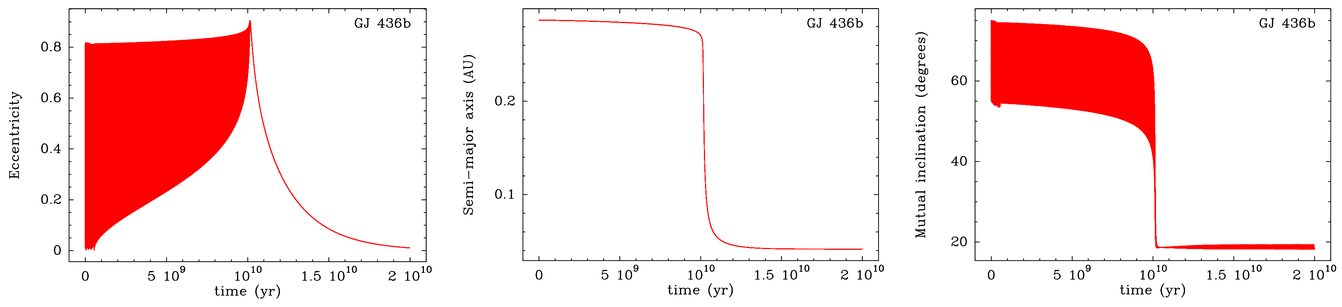

Figure 3 : Same run as in Fig. 2, but long term orbital evolution. **Left :** Evolution of GJ 436b's eccentricity evolution, showing Kozai cycles in the first phase and a smooth decrease in the second phase; **Middle :** Evolution of the semi-major axis. The orbit decays sharply at the beginning of the second phase; **Right :** Evolution of the mutual inclination between both orbits, which stabilizes at $\sim 20°$ in the second phase.

4 Exploration of the parameter space

- The secular KCTF evolution in Fig. 3 holds for a specific choice of initial parameters. Choosing other initial values always leads to a similar evolution, but over a timescale that can vary by orders of magnitudes (10^5–10^{11} yr). The key timescale is the transition time $t_{\rm tr}$ between phases 1 and 2 (~ 10 Gyr in Fig. 3). $t_{\rm tr}$ depends critically on the mass and the orbital period of the perturber (m', T'), the initial mutual inclination i_0 and the starting semi-major axis a_0 for GJ 436b.
- The KCTF scenario can account for the present orbital configuration of GJ 436b if $t_{\rm tr}$ is comparable to the age of GJ 436. We consider thus as likely every $t_{\rm tr}$ value between 1 Gyr and 10 Gyr. In Fig. 3, $t_{\rm tr}$ is actually already too long.
- Figure 4 shows a summary of the parameter space exploration. Each plot corresponds to the use of a fixed set of (a_0, i_0) values where we let parameters (T', m') vary. In regions marked "Fast Kozai", we have $t_{\rm tr} < 1$ Gyr; regions marked "slow Kozai" correspond to $t_{\rm tr} > 10$ Gyr. In regions quoted "No Kozai", the perturbation is too weak to allow the onset of Kozai cycles.
- In the middle of the plots, a convenient strip appears where $t_{\rm tr}$ falls in the desired range, with two distinct regimes. Towards low T' values (close-in perturbers), it roughly follows a $m' \propto T'^{-1/3}$ law, which can be explained by a limitation of the efficiency of the Kozai mechanism due to the small mass of the perturber. Towards high T' values, we roughly have $m' \propto T'^2$, which results from the fact that the efficiency of the Kozai migration process is controlled by the period of the Kozai cycles.
- A comparison between the location of the convenient strip in (T', m') space and the observational upper limits (photometric and radial velocities) leads to the following constraints : $70° \lesssim i_0 \lesssim 110°$ and $0.1\,{\rm AU} \lesssim a_0 \lesssim 10\,{\rm AU}$, but more probably $0.1\,{\rm AU} \lesssim a_0 \lesssim 0.5\,{\rm AU}$.
- **Provided these conditions are fullfilled, the proposed scenario can account for the present-day orbital configuration of GJ 436b**. Further monitoring of the star is therefore required to look for the suspected perturbing companion.

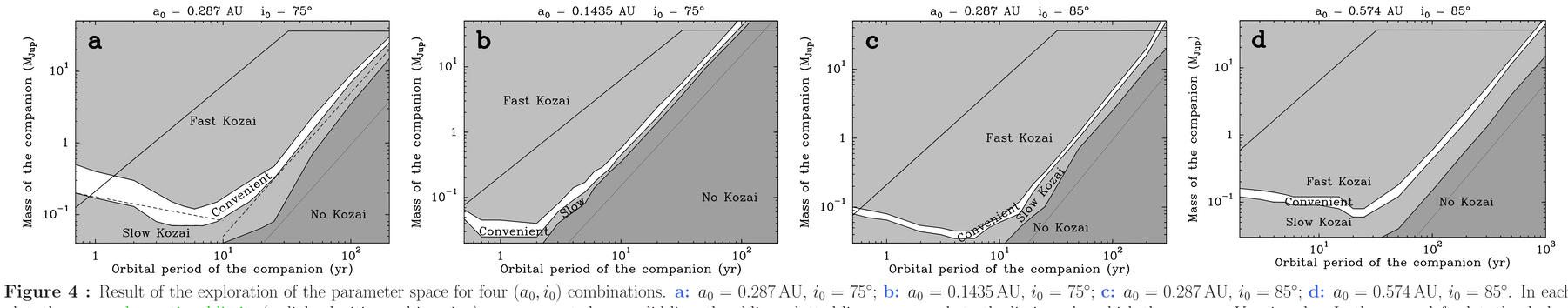

Figure 4 : Result of the exploration of the parameter space for four (a_0, i_0) combinations. **a:** $a_0 = 0.287$ AU, $i_0 = 75°$; **b:** $a_0 = 0.1435$ AU, $i_0 = 75°$; **c:** $a_0 = 0.287$ AU, $i_0 = 85°$; **d:** $a_0 = 0.574$ AU, $i_0 = 85°$. In each plot, the upper observational limits (radial velocities and imaging) are represented as a solid line; the oblique dotted line corresponds to the limit under which there are no Kozai cycles. In the upper left plot, the dashed lined are $m' \propto T'-1/3$ and $m' \propto T'^2$ power laws (see text).

References

Bailey M.E., Chambers J.E., Hahn G., 1992, A&A **257**, 315
Ballard S., Christiansen J.L., Charbonneau D., et al., 2010, ApJ **716**, 1047
Batygin K., Laughlin G., Meschiari S., et al., 2009, ApJ **699**, 23
Beust H., 2003, A&A **400**, 1129
Beust H., Bonfils X., Montagnier G., et al., 2012, A&A **545**, A88
Butler R.P., Vogt S.S., Marcy G.W, 2004, ApJ **617**, 580
Demory B.O., Gillon M., Barman T., et al., A&A **475**, 1125
Fabrycky D., Tremaine S., 2007, ApJ **669**, 1298
Gillon M., Pont F., Demory B.-O., et al., 2007, A&A **472**, L13
Kozai Y., 1962, AJ 67, 591
Maness H.L., Marcy G.W., Ford E.B., et al., 2007, PASP **119**, 90
Mardling R.A., 2008, arXiv0805.1928
Nagasawa M., Ida S., Bessho T., 2008, ApJ 678, 498
Torres G., 2007, ApJ **671**, L65